THE ASTROPHYSICAL JOURNAL, 547:L147–L150, 2001 February 1

HIGH-ENERGY X-RAY TIMING EXPERIMENT DETECTIONS OF HARD X-RAY TAILS IN SCORPIUS X-1

FLAVIO D'AMICO,[1,2] WILLIAM A. HEINDL,[1] RICHARD E. ROTHSCHILD,[1] AND DUANE E. GRUBER[1]

Received 2000 August 17; accepted 2000 November 13; published 2001 January 22

ABSTRACT

We report the detection of a nonthermal hard X-ray component from Sco X-1 based on the analysis of 20–220 keV spectra obtained with the High-Energy X-Ray Timing Experiment on board the *Rossi X-Ray Timing Explorer* satellite. We find that the addition of a power-law component to a thermal bremsstrahlung model is required to achieve a good fit in five of 16 observations analyzed. Using Proportional Counter Array data, we were able to track the movement of the source along the Z diagram, and we found that the presence of the hard X-ray tail is not confined to a specific Z position. However, we do observe an indication that the power-law index hardens with increasing $\dot{M}$, as indicated from the position on the Z diagram. We find that the derived nonthermal luminosities are ~10% of that derived for the brightest of the atoll sources.

Subject headings: binaries: general — stars: individual (Scorpius X-1) — stars: neutron — X-rays: stars

1. INTRODUCTION

Observations of hard X-ray emission from atoll sources (e.g., Barret, McClintock, & Grindlay 1996; Barret et al. 2000) have revealed the unexpected result that power-law spectra extending above 30 keV may not be an exclusive signature of a black hole. *Rossi X-Ray Timing Explorer* (*RXTE*) observations of hard X-ray emission from SAX J1808.4−3658 (Heindl & Smith 1998) demonstrated that hard X-ray flux is also present in other types of low-mass X-ray binaries (LMXBs). These observations refined the role of hard X-ray emission in distinguishing between neutron star and black hole binaries.

Scorpius X-1 is a high-luminosity LMXB Z source, where the primary is a neutron star with a low magnetic field. The presence of a nonthermal component in Sco X-1 has been suggested (e.g., Peterson & Jacobson 1966; Riegler, Bolt, & Serlemitsos 1970; Agrawal et al. 1971; Haymes et al. 1972; Duldig et al. 1983), and the absence of such a component has also been reported (e.g., Lewin, Clark, & Smith 1967; Buselli et al. 1968; Jain et al. 1973; Johnson et al. 1980). In fact, high-sensitivity searches have failed to detect such a component, placing strong upper limits on the nonthermal flux (e.g., Greenhill et al. 1979; Rothschild et al. 1980; Soong & Rothschild 1983). More recently, however, Strickman & Barret (2000) have reported the presence of a hard X-ray tail in Sco X-1 using *Compton Gamma Ray Observatory*/OSSE.

We used *RXTE* observations from the public database to search for hard X-ray tails in Sco X-1 spectra. Sco X-1 has been observed with *RXTE* several times, and our data sample (1997 April–1999 July) contains 185,672 s of Proportional Counter Array (PCA) on-source time and more than 100 ks of on-source live time in the High-Energy X-ray Timing Experiment (HEXTE). We describe data selection and analysis in § 2, describe the results in § 3, discuss the detection of a nonthermal component in § 4, and present our conclusions in § 5.

2. DATA SELECTION AND ANALYSIS

In this work, we used data from HEXTE to search for hard X-ray tails in Sco X-1 in the ~20–220 keV interval and data from the PCA to determine the Z position of Sco X-1 in the color-color diagram. The PCA (Jahoda et al. 1996) is a set of five identical xenon proportional counters covering the energy range 2–60 keV with a total area of ~7000 cm^2. The HEXTE (Rothschild et al. 1998) consists of two clusters of four NaI(Tl)/CsI(Na) phoswich scintillation counters totaling ~1600 cm^2 of effective area in the 15–250 keV energy range. Each cluster rocks between source and two background fields to measure the instrumental background in near real time. The PCA background is estimated from particle rates and the known diffuse X-ray flux. The PCA and HEXTE share a common 1° FWHM of view. Pertinent to this work, the HEXTE continuum sensitivity at 100 keV, for ~5 ks of live time, is ~13 mcrab (3 σ, scaled to in-flight backgrounds from the predictions of Gruber et al. 1996).

We selected those observations from the *RXTE* public database (as of 2000 April) in which $\gtrsim$5000 s of HEXTE total on-source time is available, in order to achieve good sensitivity at high energies. Since some observations did not point directly at Sco X-1 (in order to reduce the very high count rate), we have also discarded observations for which *RXTE* pointing offsets were larger than 0°.01. These criteria resulted in selection of the 16 observations displayed in Table 1. The resulting accumulated on-source HEXTE live time is 104,238 s.

2.1. *Data Analysis*

We performed our analysis using HEXTE Archive Histogram Mode data, which are accumulated every 16 s, have spectral information in 64 compressed channels, and are present for all observations, independent of selected science mode.

The data analysis was performed using software from FTOOLS 5.0. For each observation, we divided the data into subsets according to position on the Z diagram (see below and Table 1). We then accumulated individual source and background count histograms for HEXTE clusters A and B and added them to form a single HEXTE source and background histogram for each subset. Response matrices for HEXTE A and B were generated and added (with weights of 0.57 and 0.43, respectively, according to their effective areas).

In order to be confident that any high-energy excesses were real, we tailored our data selection to optimize background subtraction. We verified that any remaining systematic errors as a result of our procedure were small and did not affect the results. We followed the standard practices extensively studied

[1] Center for Astrophysics and Space Sciences, University of California, San Diego, 9500 Gilman Drive, La Jolla, CA 92093-0424; fdamico@ucsd.edu, wheindl@ucsd.edu, rrothschild@ucsd.edu, dgruber@ucsd.edu.

[2] Instituto Nacional de Pesquisas Espaciais, Av. dos Astronautas 1758, 12227-010 S. J. dos Campos-SP, Brazil.

TABLE 1

SELECTED *RXTE* DATA OBSERVATIONS OF SCO X-1

OBSID	MJD	Observation Number	Z Position	Live Time[a]	S/N[b]	$F_{\rm test}$[c]	Flux[d]	Hard Tail
20053-01-01-00	50,556	1	HB	6341	10.6	4.4×10^{-15}	$8.57^{+1.52}_{-1.38}$	Yes
20053-01-01-02	50,558	2	NB	5434	4.2	1.7×10^{-7}	$4.05^{+0.57}_{-0.87}$	
20053-01-01-03	50,559	3	NB	5896	4.8	3.9×10^{-9}	$5.20^{+0.75}_{-0.74}$	
20053-01-01-05	50,561	4	NB	1908	0.8	6.2×10^{-5}	$6.29^{+1.77}_{-1.77}$	No
20053-01-01-05	50,561	5	FB	4593	2.4	7.7×10^{-4}	$2.47^{+1.94}_{-1.51}$	
20053-01-01-06	50,562	6	NB	8558	7.3	3.5×10^{-13}	$8.63^{+0.91}_{-0.90}$	Yes
10061-01-03-00	50,815	7	NB	5484	4.2	2.7×10^{-9}	$5.48^{+0.69}_{-0.74}$	
20053-01-02-00	50,816	8	FB	8145	18.6	5.8×10^{-12}	$13.6^{+2.0}_{-2.0}$	Yes
20053-01-02-03	50,819	9	NB	5686	3.5	2.7×10^{-9}	$5.91^{+0.96}_{-0.95}$	
30036-01-01-000	50,820	10	FB	6858	5.8	3.8×10^{-7}	$7.73^{+1.62}_{-1.65}$	Yes
20053-01-02-04	50,820	11	FB	4193	4.9	3.3×10^{-4}	$3.44^{+1.23}_{-1.00}$	
30036-01-02-000	50,821	12	NB	4370	2.2	3.6×10^{-4}	$4.50^{+0.87}_{-0.90}$	
30036-01-02-000	50,821	13	FB	2527	1.8	3.6×10^{-4}	$2.83^{+1.05}_{-1.06}$	
30406-01-02-00	50,872	14	NB	2326	2.5	1.0×10^{-6}	$4.03^{+1.07}_{-1.13}$	
30406-01-02-00	50,872	15	FB	3125	<0	0.08	<2.20	No
30035-01-01-00	50,963	16	HB	6253	6.2	1.2×10^{-14}	$3.63^{+0.92}_{-0.88}$	Yes
30035-01-03-00	50,965	17	NB	3750	1.3	2.4×10^{-8}	$3.20^{+0.86}_{-0.89}$	
30035-01-03-00	50,965	18	FB	2318	<0	0.03	<2.67	No
30035-01-04-00	50,966	19	FB	6230	<0	0.38	<1.00	No
40706-01-01-000	51,433	20	NB	8076	2.8	1.4×10^{-5}	$2.09^{+0.55}_{-0.53}$	
40706-01-01-000	51,433	21	FB	2167	2.2	1.2×10^{-3}	$2.45^{+1.04}_{-1.07}$	

[a] Total live time for HEXTE, in units of seconds.

[b] S/N in the 75–220 keV energy range.

[c] Probability that a better fit occurred because of a random chance.

[d] Flux in the 75–220 keV energy range, in units of 10^{-10} ergs cm^{-2} s^{-1}; apart from the five detections of a hard X-ray tail, the photon index used for the nonthermal component was our average value of 1; uncertainties are given at 90% confidence level.

for HEXTE background subtraction by us and other workers (Rothschild et al. 1998; MacDonald 1999). First, we selected only data taken more than 15 minutes after satellite passage through the South Atlantic Anomaly. This allows any short-lived radioactive species produced in the detector material to decay and ensures that the systematic error of our linearly interpolated background estimate is $\lesssim$0.02% of the background. We verified this process by comparing—for each cluster—the spectra from the two separate background fields that are sampled alternately during observations. In each case, subtracting these spectra showed no excess emission, giving us confidence in the on-source background estimate. This also verified that there were no confusing sources in the background fields. We note, too, that none of the Sco X-1 spectra show evidence for the prominent instrumental background lines at ~30, 70, 160, and 190 keV (Rothschild et al. 1998), which we would expect to be apparent if there were over- or undersubtracted backgrounds. Even though there was no obvious sign of residual background features, we allowed the normalization of the background spectra to vary in our fitting procedure. As expected, the fitted adjustment to the background level was always $\lesssim$1%. Even with this added degree of freedom (dof), the significance of the detected high-energy tails remained essentially unchanged. This also verified that live times were calculated accurately, as systematic errors in the exposure would lead to incorrect background subtraction. Finally, at 100 keV (see Fig. 1), the Sco X-1 hard flux is of the order of 0.02 counts s^{-1} keV^{-1}, while the HEXTE background was typically 0.23 counts s^{-1} keV^{-1}. Thus, our measurements are at a level of ~10% of the background. MacDonald (1999) showed that our background subtraction method, even for very long integrations, is free of systematic errors at a level of ~0.05% of the background. A more detailed discussion of HEXTE background systematics is given in Gruber et al. (1996).

We used the PCA data in order to constrain the position of Sco X-1 in a color-color diagram. High-resolution (~4 ms) light curves provided power spectra to characterize any quasi-periodic oscillations and/or continuum noise. Low-resolution (16 s) light curves were used to generate color-color diagrams. We defined soft color as the ratio of the counts in the (5–7)/(3–5) keV energy bands and hard color as the ratio (7–20)/(5–7) keV. For observations 5/6, 12–15, 17/18, and 20/21 (see Table 1), the source was moving between the normal branch (NB) and flaring branch (FB). For those five dual-branch observations, we divided each into NB and FB subsets. This then resulted in 21 subsets.

2.2. *Spectral Fitting*

We used XSPEC 11.0 to fit the 20–220 keV HEXTE spectra with a combination of a *thermal* component plus a *hard* component. To fit the thermal component, we tested the following models: thermal Comptonization (e.g., Lamb & Sanford 1979), blackbody, and thermal bremsstrahlung. The thermal bremsstrahlung model returned, in all of our subsets, the smallest χ^2, and it was utilized to represent the lower energy HEXTE flux.

In the five subsets in which we detected the presence of a hard X-ray tail (see § 3), a simple power-law model, as well as ones with a spectral break, were evaluated. We found that the simple power-law model described the hard component well, and it was used to represent the higher energy HEXTE flux. In all five subsets with significant nonthermal flux, a high-temperature thermal component did not provide an acceptable fit.

3. RESULTS

We developed two criteria to determine the presence of a hard X-ray tail in a particular spectrum: (1) a signal-to-noise ratio

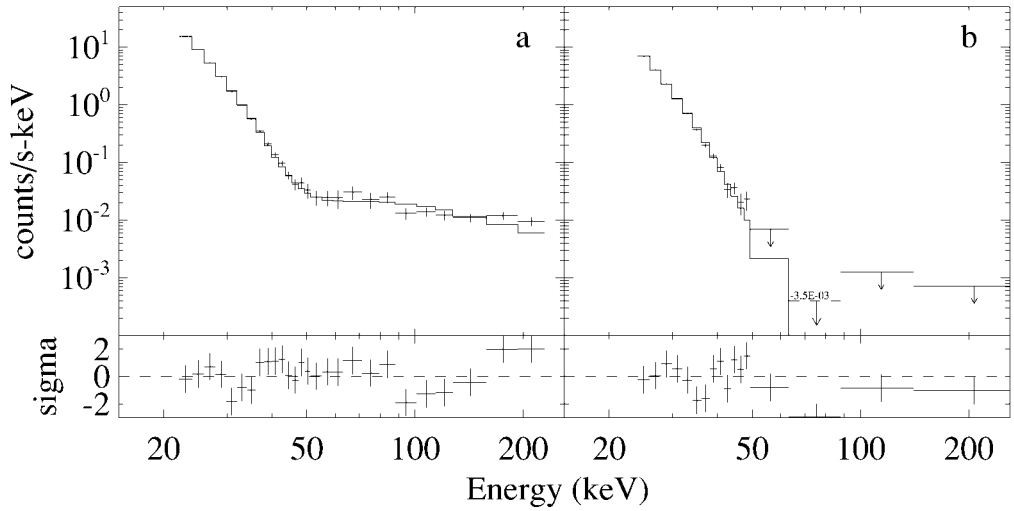

FIG. 1.—Spectrum resulting from (*a*) a bremsstrahlung + power-law fit to data subset 20053-01-02-00 and (*b*) a bremsstrahlung fit to subset 30035-01-04-00, showing the presence/absence of a hard X-ray tail in Sco X-1. Residuals are given in units of standard deviations (*bottom panels*). In (*b*) the upper limits are 2 σ, including the 60–80 keV bin, which experienced a -3 σ residual. The χ^2_ν are 1.27 and 1.62, respectively.

(S/N) $\geq$5 in the 75–220 keV energy range and (2) an *F*-test null significance for the addition of the hard component at a level of 10^{-7} or less. We claim that we observed a hard X-ray tail *only* when both these criteria were fulfilled. We thus have five strong detections of nonthermal flux in Sco X-1 spectra, with the hard X-ray tail extending at least to 220 keV. The spectral parameters derived for those subsets are shown in Table 2. Similarly, we defined a strong nondetection when (1) the S/N in the 75–220 keV range is less than 1 and (2) the *F*-test is at a level of $\gtrsim 10^{-5}$. We thus have four strong nondetections. We note that several subsets formally have very significant *F*-test values but S/N values less than 5. These typically result from deviations in the 30–50 keV range, possibly due to imperfect modeling of the thermal component. We cannot conclude that these subsets have truly nonthermal emission, although this possibility is open. In Figure 1 we show spectra from both one of our detections and one of our nondetections.

The derived photon indices (Γ) for the five subsets where the tail was observed spanned a wide range: from -0.7 to 2.4, which differs from the OSSE results, which have an average of 2.5 (Strickman & Barret 2000). It is suggestive that the two hardest photon indices were obtained when the source was on the FB and the softest were on the horizontal branch (HB), showing a possible correlation between the hardness of the spectrum and the mass accretion rate $\dot{M}$, which increases in the sequence HB $\rightarrow$ NB $\rightarrow$ FB (e.g., van der Klis et al. 1996). We also note that both times the source was on the HB a hard X-ray tail was detected.

The nonthermal 20–200 keV flux from the five detections varied by a factor of $\sim$2.5, (0.63–1.56) $\times$ 10^{-9} ergs cm^{-2} s^{-1} (see Table 2). Upper limits to the 20–200 keV flux from the four strong nondetections were estimated using a photon index of 1, the mean from the five detections. The one nondetection subset with equivalent sensitivity to the detection subsets has a 2 σ upper limit to the 20–200 keV flux of 1.0 $\times$ 10^{-10} ergs cm^{-2} s^{-1}. This implies at least an order of magnitude in overall variability in the nonthermal component in Sco X-1.

In order to estimate the 2–20 keV luminosity $L^{\rm total}_{2-20}$, we used a complex multicomponent model to heuristically fit the PCA spectra. We estimate the uncertainty in the derived flux due to uncertainties in the proper spectral shape to be $\sim$2%. Using 2.8 kpc as the distance to Sco X-1 (Bradshaw, Fomalont, & Geldzahler 1999), $L^{\rm total}_{2-20}$ is in the range (2.1–3.2) $\times$ 10^{38} ergs s^{-1} for the five detection subsets. Similarly, the range of the 20–200 keV luminosities of the nonthermal component measurements is $L^{\rm nt}_{20-200}$ = (5.9–15.0) $\times$ 10^{35} ergs s^{-1}. Thus, the nonthermal component represents about 1% of the total flux from Sco X-1.

No correlation between the *presence* of the hard tail and the position of the source in the color-color diagram is indicated; i.e., we have observed the hard X-ray tail in all three branches. In addition, the HEXTE thermal component is not correlated

TABLE 2
OBSERVATIONS OF HARD X-RAY TAIL DETECTIONS IN SCO X-1

	BREMSSTRAHLUNG		POWER-LAW		
OBSID	*kT* (keV)	Flux[a]	Γ	Flux[b]	χ^2 (dof)
20053-01-01-00	$4.83^{+0.04}_{-0.05}$	$9.03^{+0.39}_{-0.36}$	$1.75^{+0.22}_{-0.20}$	$1.56^{+0.10}_{-0.11}$	36.76 (23)
20053-01-01-06	$4.50^{+0.05}_{-0.05}$	$5.83^{+0.30}_{-0.27}$	$1.64^{+0.29}_{-0.27}$	$0.91^{+0.11}_{-0.10}$	24.52 (23)
20053-01-02-00	$4.36^{+0.03}_{-0.03}$	$7.16^{+0.26}_{-0.24}$	$-0.17^{+0.30}_{-0.33}$	$1.22^{+0.13}_{-0.14}$	29.15 (23)
30036-01-01-000	$4.28^{+0.03}_{-0.04}$	$9.63^{+0.42}_{-0.41}$	$-0.71^{+0.63}_{-0.70}$	$0.63^{+0.11}_{-0.11}$	28.57 (22)
30035-01-01-00	$4.51^{+0.08}_{-0.07}$	$7.45^{+0.60}_{-0.67}$	$2.37^{+0.33}_{-0.28}$	$1.04^{+0.08}_{-0.08}$	24.01 (22)

NOTE.—Uncertainties are given at 90% confidence level for the derived parameters of the model applied.

[a] Flux in the 20–50 keV range in units of 10^{-9} ergs cm^{-2} s^{-1}.

[b] Flux in the 20–200 keV range in units of 10^{-9} ergs cm^{-2} s^{-1}.

with the presence of the hard X-ray tail; i.e., the presence of the hard tail is indicated by neither the temperature nor flux of the HEXTE thermal component.

4. DISCUSSION

From the lack of correlation between the presence of the hard tail and the position of the source in the color-color diagram, it would appear that the hard X-ray tail emission region is not associated with that part of the accretion disk that is believed to be responsible for the quasi-periodic oscillation behavior (van der Klis et al. 1996). These results also do not support a correlation between the presence of the hard tail and clustering in the color-color diagram, such as mentioned by Strickman & Barret (2000). We also note that this behavior is different from GX 17+2, in which a hard tail is correlated with the position in the Z (Di Salvo et al. 2000). Frontera et al. (1998) have also reported the detection of a hard tail in another Z source (Cyg X-2).

Nevertheless, we must point out that the observed photon indices may be related to the position in the Z diagram. The hardest observed photon indices are in the FB and the softest ones in the HB. From this point of view, the production of hard X-ray photons may be correlated with the accretion rate at the inner part of the disk. Motivated by the observation that Sco X-1 is a variable radio source (e.g., Fender & Hendry 2000), we considered whether or not the hard X-ray emission could be explained in terms of synchrotron emission. While the measured photon indices are consistent with this idea for the HB and NB, the ones measured when the source was in the FB (consistent with 0) are not, since it would require an inverted distribution of relativistic electrons. Similarly, the HB and NB spectra could result from Comptonization, but the FB power-law indices are again too hard.

A difference between atoll sources and Sco X-1 is also seen in the soft X-ray luminosity. The atoll source hard tails appear when the 2–20 keV luminosity is relatively low, less than 10^{37} ergs s^{-1}; whereas the soft flux in Sco X-1 is essentially at the Eddington limit ($\sim 10^{38}$ ergs s^{-1}). It is also interesting to note that some models used to explain the hard X-ray emission of atoll LMXBs (e.g., Mitsuda et al. 1989; Hanawa 1990) are applicable in a low-luminosity state up to ~20 keV. This, however, is not the case of our observations. On the other hand, Sco X-1 may be similar to some atoll sources in the luminosity of the power-law component. The Sco X-1 power-law luminosity in the 20–200 keV range is comparable to the weaker atoll source hard X-ray luminosities reported by Barret et al. (1996).

Distinguishing neutron stars from black holes remains a key goal in high-energy astrophysics. Recently it has been argued (Barret et al. 2000) that the luminosities in the 1–20 keV (defined as $L_{\rm X}$) and 20–200 keV (defined as $L_{\rm HX}$) bands could be used to distinguish between black hole and low-state neutron star systems displaying hard X-ray emission. In their argument, the critical luminosity, $L_{\rm crit} = 1.5 \times 10^{37}$ ergs s^{-1}, is the dividing line between neutron star and black hole binaries with the neutron star systems emitting $L_{\rm HX} \sim L_{\rm X}$ when $L_{\rm X} \lesssim L_{\rm crit}$. Since Sco X-1 is emitting Eddington-level soft fluxes, we cannot test that idea. On the other hand, our observed $L_{\rm HX}$ does not contradict the idea pointed out by Barret et al. (2000) that only black hole binaries can have both $L_{\rm X}$ and $L_{\rm HX}$ above $L_{\rm crit}$, since our measured $L_{\rm HX}$ is below the value of $L_{\rm crit}$ (see Table 1).

5. CONCLUSION

We have observed significant detections of a nonthermal component in Sco X-1 on five out of 21 occasions with HEXTE on board *RXTE*. We also have found that the presence of the hard X-ray tail is not associated with a particular position in the color-color diagram, but that the photon indices, instead, may be correlated with the position on the Z diagram, albeit with a very limited number of examples. We inferred that the nonthermal power-law flux of the source varied by over an order of magnitude comparing our detections with the nondetections and by a factor of ~3 in the five cases where the presence of the hard X-ray tail was strongly indicated. Our observed 20–200 keV luminosities are in agreement with only black hole binaries emitting hard X-rays with luminosity $\gtrsim 1.5 \times 10^{37}$ ergs s^{-1}.

This research has made use of data obtained through the HEASARC, provided by the NASA/Goddard Space Flight Center. F. D. gratefully acknowledges FAPESP/Brazil for financial support under grant 99/02352-2. F. D. acknowledges Stefan Dieters, Wayne Coburn, and John Tomsick for helpful discussions. We also thank an anonymous referee for suggestions. This research was supported by NASA contract NAS5-30720.

REFERENCES

Agrawal, P. C., Biswas, S., Gokhale, G. S., Iyengar, V. S., Manchanda, R. K., & Sreekantan, B. V. 1971, Ap&SS, 10, 500
Barret, D., McClintock, J. E., & Grindlay, J. E. 1996, ApJ, 473, 963
Barret, D., Olive, J. F., Boirin, L., Done, C., Skinner, G. K., & Grindlay, J. E. 2000, ApJ, 533, 329
Bradshaw, C. F., Fomalont, E. B., & Geldzahler, B. J. 1999, ApJ, 512, L121
Buselli, G., Clancy, M. C., Davison, P. J. N., Edwards, P. J., McCracken, K. G., & Thomas, R. M. 1968, Nature, 219, 1124
Di Salvo, T., et al. 2000, 544, L119
Duldig, M. L., Greenhill, J. G., Fenton, K. B., Thomas, R. M., & Watts, D. J. 1983, Ap&SS, 95, 137
Fender, R. P., & Hendry, M. A. 2000, MNRAS, 317, 1
Frontera, F., et al. 1998, Nucl. Phys. B, 69, 286
Greenhill, J. G., et al. 1979, MNRAS, 189, 563
Gruber, D. E., Blanco, P. R., Heindl, W. A., Pelling, M. R., Rothschild, R. E., & Hink, P. L. 1996, A&AS, 120, 641
Hanawa, T. 1990, ApJ, 355, 585
Haymes, R. C., Harnden, F. R., Jr., Johnson, W. N., III, Prichard, H. M., & Bosch, H. E. 1972, ApJ, 172, L47
Heindl, W. A., & Smith, D. M. 1998, ApJ, 506, L35
Jahoda, K., Swank, J. H., Giles, A. B., Stark, M. J., Strohmayer, T., Zhang, W., & Morgan, E. H. 1996, Proc. SPIE, 2808, 59
Jain, A. K., Jayanthi, U. B., Kasturirangan, K., & Rao, U. R. 1973, Ap&SS, 21, 107
Johnson, W. N., Kurfess, J. D., Maurer, G. S., & Strickman, M. S. 1980, ApJ, 238, 982
Lamb, P., & Sanford, P. W. 1979, MNRAS, 188, 555
Lewin, W. H. G., Clark, G. W., & Smith, W. B. 1967, ApJ, 150, L153
MacDonald, D. R. 1999, Ph.D. thesis, Univ. California, Riverside
Mitsuda, K., Inoue, H., Nakamura, N., & Tanaka, Y. 1989, PASJ, 41, 97
Peterson, L. E., & Jacobson, A. S. 1966, ApJ, 145, 962
Riegler, G. R., Boldt, E., & Serlemitsos, P. 1970, Nature, 226, 1041
Rothschild, R. E., et al. 1980, Nature, 286, 786
———. 1998, ApJ, 496, 538
Soong, Y., & Rothschild, R. E. 1983, ApJ, 274, 327
Strickman, M., & Barret, D. 2000, in AIP Conf. Proc. 510, Proc. Fifth Compton Symposium, ed. M. L. McConnell & J. M. Ryan (New York: AIP), 222
van der Klis, M., Swank, J. H., Zhang, W., Jahoda, K., Morgan, E. H., Lewin, W. H. G., Vaughan, B., & van Paradijs, J. 1996, ApJ, 469, L1